Directional K^+ Channel insertion in a single phospholipid bilayer: Neutron Reflectometry and Electrophysiology in the joint exploration of a model membrane functional platform.

V. Rondelli[1], E. Del Favero[1], P. Brocca[1], G. Fragneto[4], M. Trapp[5], L. Mauri[1], M.G. Ciampa[1], G. Romani[2], C.J. Braun[3], L. Winterstein[3], I. Schroeder[3], G. Thiel[3], A. Moroni[2], L. Cantu'[1]

[1] Dept. of Medical Biotechnologies and Translational Medicine, University of Milan, Italy

[2] Dept. of Biosciences, University of Milan and Institute of Biophysics, Consiglio Nazionale delle Ricerche, CNR, Milano, Italy

[3]Dept. Biology, Technische Universität Darmstadt. Schnittspahnstraße 3. 64287 Darmstadt, Germany

[4] Institut Laue-Langevin, 71 avenue des Martyrs, BP 156, 38000 Grenoble Cedex, France

[5] Helmholtz-Zentrum Berlin für Materialien und Energie, Institute for Soft Matter and Functional Materials, Hahn-Meitner-Platz 1, 14109 Berlin, Germany

CORRESPONDING AUTHOR:

Laura Cantu'

Dept. of Medical Biotechnologies and Translational Medicine, University of Milan

LITA - Via Fratelli Cervi, 93, 20090 Segrate (Milano)

Tel: +390250330362; Fax: +390250330365

e-mail: laura.cantu@unimi.it

Abstract

We investigated the insertion of small potassium (K^+) channel proteins ($Kcv_{MA\text{-}1D}$ and Kcv_{NTS}) into model membranes and the lipid-protein structural interference, combining neutron reflectometry and electrophysiology. Neutron reflectometry experiments showed how the transverse structure and mechanical properties of the bilayer were modified, upon insertion of the proteins in single model-membranes, either supported on solid substrate or floating. Parallel electrophysiology experiments were performed on the same channels reconstituted in free-standing planar lipid bilayers, of both typical composition and matched to the neutron reflectometry experiment, assessing their electrical features. Functional and structural results converge in detecting that the proteins, conical in shape, insert with a directionality, cytosolic side first. Our work addresses the powerful combination of the two experimental approaches.. We show here that membrane structure spectroscopy and ion channel electrophysiology can become synergistic tools in the analysis of structural-functional properties of biomimetic complex environment.

KEYWORDS: neutron reflectivity, phospholipids, potassium channels, protein-lipid interaction, protein reconstitution

1. INTRODUCTION

The complex structure arising from the interaction of membrane proteins with membrane lipids involves the chemico-physical properties of both. Nonetheless, it is far from being the mere superposition of the features of individual components, rather, true structural interference is likely to occur [1]. From the membrane side, parameters such as the hydrophobic thickness of the lipids, the lateral pressure field of the membrane, the distribution of charges at the protein–lipid interface, the membrane composition are likely to play a role [2]. From the protein side, the interaction is affected by the presence and properties of specifically localized amino acid side chains in relation to the lipid bilayer [3-6]. Protein–lipid interactions can be critical for correct insertion, folding, and topology of membrane proteins [7,8]. Specific interactions between the polar region of phospholipid heads and charged amino acids could help guiding membrane protein orientation [9]. Moreover, changes in lipid composition can reversibly affect membrane-protein topology.

The use of simplified model systems, coupled with appropriate techniques, can help in clarifying some of the aforementioned aspects.

In the present study we focus on two aspects, the directionality of protein inclusion and the bilayer structural changes, by studying a very simple model, namely the insertion of minimal channel-proteins into single planar monocomponent phospholipid membranes. This model is suitable for parallel observation by neutron reflectivity and electrophysiology, with the potentiality of unraveling the connection between the cross structuring of the protein / membrane system and its functionality

Ion channels are a class of ubiquitous membrane proteins in organisms. They are amenable for structure-function analysis because they can be inserted in model membranes where their activity can be detected because they generate a measurable electrical current, in the orders of pA. Functional reconstitution of ion channels into planar lipid bilayers is a well-established method in electrophysiology [10,11] with the advantage of reducing the system to its minimal components,

lipids and membrane proteins, besides allowing the study of ion channels found in intracellular organelles, hardly accessible by patch clamp pipettes [12,13]. Insertion of ion channels in planar bilayers is usually obtained by fusing proteoliposomes to one side of the bilayer by means of an imposed osmotic gradient [14-17]. A drawback of this method is that it does not provide control over the orientation of the protein, which can presumably insert in the bilayer in two different ways, by the cytosolic or by the extracellular side. Hence, it is difficult to correlate the properties of an ion current, measured in the bilayer, with the physiologically relevant direction of current flow in a cell or an organelle. Moreover, the structural response of the lipid bilayer occurring upon protein insertion cannot be accessed by the electrophysiological techniques (unless they induce changes in the current behaviour), and is mainly unexplored and overridden.

On the other hand, the cross structure of a membrane where a protein is inserted can be assessed by neutron reflectometry. This technique measures the reflected intensity of a highly collimated neutron beam from a membrane laying on a surface, treated as a stack of stratified mirrors, finally allowing for the reconstruction of its cross compositional profile [18]. Moreover, neutron investigation can take advantage of the peculiar H-D isotope different contrast, providing an enhanced visibility of even small amounts of a protiated macromolecule embedded into a deuterated hosting environment, and allowing to define its location [19-23]. A particular experimental configuration is of interest in our case, consisting of a floating single membrane freely suspended in water [24].

We use here a class of ion channels that, to date, represent the smallest functional potassium (K+) channels identified in nature. $Kcv_{MA\text{-}1D}$ and Kcv_{NTS} belong to the Kcv-like family of channels identified in viruses. These channels assemble into functional tetramers of identical subunits. Each subunit is composed by two transmembrane domains connected by a pore loop. A main plus for the present work is that both $Kcv_{MA\text{-}1D}$ and Kcv_{NTS} have a conical structure [25,26] and a well-established current-voltage (I/V)-relation [27,28]. Moreover, the assignment of the orientation of

these channels reconstituted in the bilayer can be indirectly deduced from the pronounced outward rectification of their current-voltage relationships.

With the aim of making an advance to structure-function connection, starting from the standard experimental conditions of either the reflectometry or electrophysiology techniques, we came to a shared model of a free membrane of given phospholipid composition. The two approaches provided the individual typical description of the systems, structural or functional, and notably converge in detecting the directional insertion of the channel into the membrane. We then show that membrane structure spectroscopy and ion channel electrophysiology can become synergistic tools in the analysis of structural-functional properties of biomimetic complex environment.

2. MATERIAL AND METHODS

2.1 Lipids and chemicals

Deuterated lipids (1,2-dimyristoyl-*sn*-glycero-3-phosphatidylcholine, d_{63}-DMPC; 1,2-distearoyl-*sn*-glycero-3-phosphatidylcholine, d_{83}-DSPC; 1,2-dipalmitoyl-*sn*-glycero-3-phosphatidylcholine, d_{75}-DPPC and d_{62}-DPPC), deuterated dodecylphosphocholine-d_{38}, (DPC-d_{38}), DPPC and 1,2-diphytanoyl-*sn*-glycero-3-phosphocholine (DPhPC) were purchased from Avanti Polar Lipids. L-α-phosphatidylcholine (type IV-S. = 30% TLC) was from Sigma-Aldrich (Steinheim, Germany). Enzymes for molecular biology were obtained from New England Biolabs or Stratagene. The detergent n-dodecyl β-D-maltoside (DDM) was from Glycon (Berlin). n-decan was from Carl Roth, Karlsruhe, Germany. Chloroform for CBB was from AppliChem (Darmstadt, Germany). All other chemicals were from Carl Roth, Karlsruhe, Germany.

2.2 Ion channel proteins for reconstitution in bilayers

We used two types of K^+ channels, the $Kcv_{MA\text{-}1D}$ channel (94 amino acids) [27] and the smaller Kcv_{NTS} channel , which is composed of only ,82 amino acids [29].

2.3 Protein expression in Pichia pastoris

The Kcv_{MA-1D} and Kcv_{NTS} genes [27, 30] were commercially synthesized to optimize codon usage for *P. pastoris* expression. A purification tag containing 7His and a proteolytic cleavage site for H3C was added in frame at the N terminus. The construct was subcloned into *P. pastoris* expression vector pPIC3.5K (Invitrogen) by standard molecular biology technique. The protease-deficient *P. pastoris* strain SMD1163 (his4, pep4, prb) (Invitrogen) was used for the expression of the K^+ channel gene. Cell growth and membrane preparation were performed as previously described [27].

2.4 Purification of Kcv proteins from *Pichia pastoris*

Membranes from cells expressing the Kcv gene constructs were detergent-solubilised in buffer (A): (40 mM imidazole, pH 7.5, 600 mM NaCl, 200 mM KCl) + DDM 60 mM, for 4 hours at 4ºC and cleared by centrifugation (100,000g, 1 hour at 4°C). The supernatant was added to Co^{2+}-Affinity resin (Sigma-Aldrich) pre-equilibrated with buffer (A) and kept in mild agitation over night at 4°C. The resin was then collected by centrifugation and packed in a column. The column was washed at 500 µL/min, three times with buffer (A) + DDM 2 mM, three times with a buffer containing 50 mM imidazole, pH 7.5, 200 mM KCl, 1M NaCl, + DDM 2 mM, and three times with buffer (A) without DDM. To recover bound protein, the column was eluted at 0.3mL/min with a buffer containing 300 mM imidazole, pH 7.5, 200 mM KCl + DDM 2 mM. The fractions of the column containing the protein were then concentrated to ca. 200 µL by using Ultracel 30K (Amicon). The protein was further purified by size exclusion chromatography with a buffer containing: 50 mM Tris/HCl, 50mM KCl and DDM 0.5 mM.

The tetrameric ensemble of Kcv-channel ($Kcv_{PBCV-1b}$ [28], 95% sequence identity to Kcv_{MA-1D}) is shown in Figure 1. The channel structure [31] was obtained from extensive molecular dynamics simulations [32] and is visualized by UCSF Chimera software [33].

2.5 Dialysis

In order to avoid aggregation and precipitation, Kcv_{MA-1D} emerging from the extraction and purification procedure is kept in solution by a solubilizing agent, namely the single-chain

amphiphile n-dodecyl β-D-maltoside (DDM). When a protein is suspended and then delivered to a membrane, the detergents can affect the membrane structure and phase, the protein functionality and the membrane-protein interaction. Solubilizers should then be carefully chosen and treated. Their interference with both membranes and proteins is far from being trivial and has been widely studied by different approaches [34-40]. Moreover, although some membrane proteins are functional in detergent environments, detergents are frequently destabilizing and can lead to inactivation of the protein over time, so that there is a research field devoted to the development of alternative solutions such as the use of peptides, amphiphols and other surfactants [41]. Recently, it has been pointed out that the solubilization of hydrophobic protein and their facilitated release to lipid membranes are competing requirements that can be matched with a low mole fraction of detergent per protein (one or two amphiphile molecules per protein) [42]. Then, a protocol of dialysis was set up, aimed at detergent minimization. Moreover, detergent substitution was also performed, with an optimal solubilizer to our purpose, namely, the fully deuterated dodecylphosphocholine-d_{38} (DPC-d_{38}), carrying the same phosphocholine polar headgroup of membrane phospholipids. Minimization and mimesis of the detergent were implemented with the aim of optimizing channel delivery meanwhile removing the impact of solubilizer on the membrane structure. Deuterated lipids were used to improve $Kcv_{MA\text{-}1D}$ channel visibility in the membrane. In fact, after protein-membrane interaction, the presence of H-atoms within the lipid bilayer could only be caused by the presence of the $Kcv_{MA\text{-}1D}$ protein, or penetrating water molecules. 1 mL of each protein solution at the concentration of 0.4 mg/mL was dialyzed. A detailed description of the protocol is reported in the Supplementary Material, together with a thin layer chromatography (TLC) slab showing both that the protein was still suspended in the final solution and that the residual detergent content was very low, below the limit of detection. TLC analysis was performed at different delays during dialysis.

Notably, as an essential requisite, after dialysis the channel activity was still maintained, as verified by functional reconstitution in a planar lipid bilayer, as described below.

2.6 Model membranes build-up

2.6.1 Multilamellar membranes

Phospholipid multilamellar aggregates were prepared in deionized water according to a standard protocol, to the final concentration of 25 mg/mL [43,44].

2.6.2 Supported membranes

Solid supports were single crystals of silicon (5 x 5 x 1.5 cm^3) polished on one large face (111). The surfaces were cleaned before use with a series of solvents, namely chloroform, acetone, ethanol, pure water, in this sequence, and then treated with plasma cleaner.

Supported membranes A, B, C and D were obtained by vesicle fusion, a widely used technique for the deposition of symmetric lipid membranes composed by selected phospholipids, applicable to neutron reflectivity measurements [18,43,45]. In order to be more sensitive to the presence of small amounts of protein, we used deuterated phospholipids and we optimised the preparation conditions to obtain good bilayers in terms of both membrane stability and surface coverage. Monodisperse lipid vesicles (~100 nm in diameter) were obtained from the multilamellar samples by extrusion on twinned 80 nm polycarbonate filters, with a manual extruder (LiposoFast, Avestin Inc.). The preparations were then stored at 45°C, above the phospholipid chains gel-to-fluid transition, to ensure vesicle stability.

After adjusting the ionic strength of the solutions to 100 mM NaCl, vesicles were incubated in the measuring cell for about 30 minutes at 40°C. Vesicle fusion and bilayer formation on the solid support were checked every 15 minutes by neutron reflectivity measurements. After bilayer formation the cell was thoroughly rinsed with deionised water to flush the excess vesicles and NaCl.

2.6.3 Floating membrane

The floating-membrane sample was deposited via Langmuir films of desired composition. Fully deuterated phospholipids were dissolved in chloroform to a final concentration of 1 mg/mL. Langmuir depositions were carried out on a Langmuir trough (NIMA, UK), filled with pure water, processed in a Milli-Q system (Millipore, Bedford, MA) to a resistivity of 18 MΩxcm, and kept at

T = 15°C (±0.5). Lipids were spread on the water surface to obtain monolayers. A full description of the coupled Langmuir-Blodgett [46] / Langmuir-Schaefer [47] techniques adapted for the used depositions is reported in [48].

2.7 Neutron Reflectometry

Reflectivity measurements from membranes A, B, C and E were performed on the D17 reflectometer at ILL [49] (Grenoble, France, TOF mode, $2 < \lambda < 20$ Å, with two incoming angles, 0.7° and 4°), whereas reflectivity measurements from membrane D were performed on the V18 reflectometer at HZB [50] (Berlin, Germany TOF mode, $2 < \lambda < 12$ Å, with three incoming angles, 0.5°, 1° and 2.8°, and constant wavelength resolution $\Delta\lambda/\lambda = 5\%$). All the sample cells were oriented vertically and kept in position while changing solvents and temperature. Measurements were performed at the silicon-water interface, the beam coming from the side of the silicon block.

In a neutron reflectivity measurement, the intensities of the reflected and incoming beams are collected and their ratio is displayed as a function of q_z, the momentum transfer perpendicular to the interface [51]. Details of the technique are reported in the Supplementary Material.

Initial characterization of the five target membranes was performed by combined reflectivity measurements in two different contrast solutions, namely H_2O (Milli-Q system) and D_2O (99% pure, Sigma). This procedure allows for full characterization of the system, as the same structural values, pertinent to the same membrane, are deduced from combined fit of different experimental spectra. After protein-membrane interaction, measurements were carried out in both in H_2O, where best contrast of the hosting deuterated membrane is obtained, and in D_2O-based solvents, providing the best visibility of the hosted protein. Fits of the different spectra, obtained upon solvent substitution, had to agree on the same membrane composition, giving further confidence to the results.

2.8 Functional reconstitution method

For the functional reconstitution of Kcv channels, we used the purified $Kcv_{MA\text{-}1D}$ protein, which was

expressed in *P.pastoris*. The Kcv_{NTS} proteins were obtained by in vitro translation and subsequent isolation as described previously [29]. The function of the channel protein was tested in planar lipid bilayers, as described previously [52]. Bilayers were formed with the Montal-Müller technique [10] with a 0.4 mg/mL solution of either L-α-phosphatidylcholine or DPhPC in n-decan. The experimental solution contained 100 mM KCl both in the *cis* and *trans* chamber and was buffered to pH7 with 10 mM HEPES/KOH. All experiments were performed between 20 and 25°C. The Ag/AgCl electrodes were connected to a head-stage of a patch-clamp amplifier (L/M-EPC 7, List–Medical, Darmstadt, Germany). Single-channel currents were filtered at 1 kHz and digitized with a sampling interval of 280 µs (3.57 kHz) by an A/D-converter (LIH 1600, HEKA Electronik, Lambrecht, Germany).

Single channel currents in DPPC bilayers were also measured with the contact bubble bilayer (CBB) technique [53] because this phospholipid did not form stable bilayers in a conventional planar lipid bilayer set up. For CBB recordings, two borosilicate glass pipettes (Kimble Chase, Gerresheimer, Vineland, USA) with a tip diameter of $\leq$ 30 µm were filled with measuring solution containing 100 mM KCl, 10 mM Hepes / pH7, 16.4 mg/ml DPPC liposomes and nano-discs containing Kcv_{NTS}. Kcv_{NTS} was expressed as reported previously [54] into nano-discs with 1,2-dimyristoyl-*sn*-glycero-3-phosphocholine (DMPC) lipids according to the manufacturer's instructions (MembraneMax^{TM} *HN* Protein Expression Kit, Invitrogen, Carlsbad (CA) USA). It is important to note that the channel protein is after reconstitution no longer determined by the lipids of the bilayer but by those of the final target bilayer

For the production of liposomes, DPPC was dissolved in 1 ml of Chloroform, dried in a glass vial and finally resolved in 10 ml measuring solution, then sonicated at ~45°C for at least one hour until it was transparent. Small "water bubbles", that is, drops of measuring solution carrying phospholipid monolayers on the surface, were formed at the two pipette tips immersed in a hexadecane medium, by applying pressure to both pipettes. After manoeuvring the individual "bubbles" together on an inverted microscope (Eclipse TS 100, Nikon), a bilayer was formed in the

area of contact. The glass pipettes were connected via Ag/AgCl electrodes with an amplifier (3900A Integrating Patch Clamp, Dagan, Minneapolis, MN, USA) for a recording of channel activity. Currents were filtered at 1 kHz and digitized with a sampling frequency of 10 kHz by an A/D converter (Instrutech LIH 8+8 data acquisition system, HEKA Electronik, Lambrecht, Germany). Data analysis was performed with KielPatch (version 3.20 ZBM/2011) and Patchmaster (HEKA Electronik, Lambrecht, Germany).

3 RESULTS AND DISCUSSION

3.1 Neutron reflectometry

Neutron reflectrometry experiments were performed on deposited membranes,both bare and after contact with the solution containing the dialyzed proteins. Preliminarly, DSC measurements had shown that coincubation of the lipid and the channel proteins produced a modification in the membrane, with an effect compatible with other cases reported in the literature [55] regarding inclusion of similar amounts of proteins in membranes (see Supplementary Material). This suggested that effective protein insertion could occur.

Then, we applied neutron reflectometry to five model phospholipid membranes.,four supported on solid substrate and one floating, as described in the Methods section. Out of the four supported single-lipid membranes, two were composed of d_{63}-DMPC (C14 chain length, fully deuterated, membranes A and B), one of d_{75}-DPPC (C16 chain length, fully deuterated, membrane C) and one of d_{62}-DPPC (D-chains, H-headgroup, membrane D). The floating membrane was composed of d_{75}-DPPC (membrane E), on top of a supported d_{83}-DSPC bilayer. Reflectivity measurements were carried out at a temperature higher than the melting transition of the lipid chains of the target membranes, namely, 40°C for the two d_{63}-DMPC membranes, and at 45°C for both floating and supported DPPC membranes. We underline that at 45°C, d_{83}-DSPC is in the gel phase, which helps in preserving the stability of the supporting membrane of the floating membrane E during a long

experiment. Reversely, the floating membrane E itself, the one exposed to channel insertion, is in the fluid phase.

Full initial characterization of the target membranes was performed by combined reflectivity measurements in different contrast solutions, as described in the Methods section. Tables 1 and 2 report, in the left block, the structural parameters corresponding to the best fits of the reflectivity curves obtained for the different target membranes, prior to protein incubation.

The thicknesses of the supported DMPC and DPPC membranes (A, B, C and D) are seen to be roughly the same, 43-44-45 Å, despite the fact that the chains of DPPC are two-carbons longer than those of DMPC. A smaller value than expected for the thickness of a deposited DPPC bilayer has been reported in the literature and has been attributed to DPPC chains tilting of about 30° due to the presence of the rigid support [56,57]. In contrast, the DPPC membrane E, floating on an underlying membrane, decoupling it from the solid support, was here measured to span a thickness of 50 Å, some 10% higher than what expected for DPPC bilayers at similar temperature [58]. Thickness overestimation is expected, as deriving from floating membrane ondulations [59,60], giving rise to an apparent membrane thickness higher than the effective..

After characterization of the target membranes, 10 μL of solution containing 0.4 mg/mL of either the $Kcv_{MA\text{-}1D}$ or the Kcv_{NTS} channel was injected into each measuring cell. For membranes A, C, D and E, the final protein:phospholipid molar ratio was 1:100. For membrane B, the protein:phospholipid content was doubled, namely 1:50. After 1 hour incubation, pure H_2O was extensively flushed, before measuring reflectivity. After measurements in H_2O, a D_2O-based solvent was flushed in each sample cell, and reflectivity was measured again. The reflectivity spectra obtained in the different solvents are shown in the Supplementary Material, together with their best fits, obtained with the parameters reported in Tables 1 and 2. Fit parameters have been obtained by a combined fit of the measurements performed with the different contrasting solvents using the program Motofit [61]. The corresponding transmembrane scattering length density profiles in H_2O or D_2O (see also Supplementary Material) are reported in Fig. 2 and 3.

A water layer between the silicon and the supported membranes, in the order of few Å, has always been observed. After protein incubation, a slight change (±1 Å) in the thickness of this water layer may occur (A: 3Å; B: 3→2Å; C: 2→1Å; D: 3→4Å; E: 2Å)

Table 1 Physical parameters corresponding to the best fits of the reflectivity curves of the membranes investigated before and after Kcv channel protein incubation. Combined best fits in different contrast solvents were performed. T: layer thickness (Å); $\rho_l(z)$: average scattering length density of the non-water components of the layer (10^{-6} Å^{-2}); W: percent water content of the layer (% in volume); r: roughness between one layer and the adjacent previous one (Å).

			Naked membrane				**Membrane + channel**					
			T	**$\rho_l(z)$**	**W**	**r**	**T**	**$\rho_l(z)$**	**W**	**r**	**channel (%vol)**	**Out/in channel ratio**
A	**d_{63}DMPC + $Kcv_{MA\text{-}1D}$**	**Heads out**	8±1	*3.54±0.02*	26±5	6±2	9±1	***3.43±0.02***	28±5	7±1	***7%***	***1.17***
		Chains out	14±1	*7.4±0.01*	20±5	3±2	14±1	***7.07±0.01***	20±5	3±2	***7%***	
		Chains in	14±1	*7.4±0.01*	20±5	7±1	14±1	***7.05±0.01***	20±4	7±2	***6%***	
		Heads in	7±1	*3.54±0.02*	26±5	5±2	7±1	***3.45±0.02***	28±5	5±2	***6%***	
B	**d_{63}DMPC + $Kcv_{MA\text{-}1D}$ 2x**	**Heads out**	8±1	*3.54±0.02*	16±5	6±2	9±1	***3.25±0.02***	20±5	8±2	***18%***	***1.17***
		Chains out	14±1	*7.4±0.01*	10±5	3±2	14±1	***6.4±0.01***	10±4	6±2	***18%***	
		Chains in	14±1	*7.4±0.01*	10±5	5±2	14±1	***6.6±0.01***	10±4	3±2	***15%***	
		Heads in	7±1	*3.54±0.02*	16±5	5±2	7±1	***3.3±0.02***	20±5	5±2	***15%***	
C	**d_{75}DPPC + $Kcv_{MA\text{-}1D}$**	**Heads out**	8±1	*4.98±0.02*	37±5	8±2	9±1	***4.83±0.02***	39±5	8±2	***5%***	***1.25***
		Chains out	15±1	*7.11±0.01*	30±5	4±2	14±1	***6.8±0.01***	30±5	3±1	***5%***	
		Chains in	15±1	*7.11±0.01*	30±4	3±2	15±1	***7±0.01***	30±5	3±2	***4%***	
		Heads in	6±1	*4.98±0.02*	35±5	5±2	6±1	***4.92±0.02***	38±5	4±2	***4%***	
D	**d_{62}DPPC + Kcv_{NTS}**	**Heads out**	9±1	1.93±0.04	28±5	2±2	8±1	1.94±0.04	28±5	2±2		***1.2***
		Chains out	15±1	*7.11±0.02*	20±5	3±2	15±1	***6.5±0.02***	20±5	4±1	***12%***	
		Chains in	14±1	*7.11±0.02*	20±4	4±2	14±1	***6.6±0.02***	20±5	3±2	***10%***	
		Heads in	7±1	1.93±0.04	28±5	3±2	7±1	1.94±0.03	28±5	2±2		

Table 2 Physical parameters corresponding to the best fits of the reflectivity curves of Membrane E, composed by d_{75}-DPPC floating over a supporting d_{83}-DSPC, before and after Kcv channel protein incubation. T: layer thickness (Å); ρ_l (z): average scattering length density of the non-water components of the layer (10^{-6} Å^{-2}); W: percent water content of the layer (% in volume); r: roughness between one layer and the adjacent previous one (Å).

		Membrane E				**Membrane E + Kcv$_{MA-1D}$**					
		T	**ρ_l(z)**	**W**	**r**	**T**	**ρ_l(z)**	**W**	**r**	**channel (%vol))**	**Out/in channel ratio**
Floating membrane (d_{75}-DPPC)	**Heads out**	9±1	*4.98±0.02*	22±5	6±2	8±1	***4.39***±*0.02*	30±5	9±2	***20%***	***1.25***
	Chains out	*18*±1	*7.11±0.01*	17±4	8±2	***15***±1	***6.1***±*0.01*	22±5	9±2	***20%***	
	Chains in	*17*±1	*7.11±0.01*	17±5	8±2	***15***±1	***6.3***±*0.01*	22±5	9±2	***16%***	
	Heads in	6±1	*4.98±0.02*	22±5	5±2	6±1	***4.5***±*0.02*	29±5	9±2	***16%***	
water		18±1			5±1	19±1			9±2		
Supporting membrane (d_{83}-DSPC)	**Heads out**	9±1	4.98±0.02	17±5	8±2	9±1	4.98±0.02	22±5	9±2		
	Chains out	23±1	7.96±0.01	9±5	3±2	23±1	7.96±0.01	14±5	7±1		
	Chains in	23±1	7.96±0.01	9±5	3±2	23±1	7.96±0.01	14±4	4±2		
	Heads in	6±1	4.98±0.02	17±5	4±2	7±1	4.98±0.02	22±5	7±2		

Several piece of information can be gained from the collected reflectivity data.

Kcv channel proteins were effectively delivered to the membranes. The first observation is that the SLD profiles of the five model-membranes changed after interaction, showing that a compositional alteration occurred. A further observation is that the SLD of the transverse section of each of the five tested membranes decreases, indicating that the non-deuterated protein entered and crossed the deuterated-lipids bilayers (see tables 1and 2).

Analysis of the spectra collected in different contrast solvents (see Supplementary Material) helps discriminating whether the SLD modification is due to protein insertion or to H_2O penetration, a main concern in H-D-contrast neutron spectroscopy experiments. Of course, it cannot be excluded that some solvent penetration was induced by the protein itself. Such a water income was evident in

the case of the floating membrane E, where a 5% solvent volume penetration increase was estimated after protein-membrane interaction. Interestingly, when a doubled amount of protein was incubated (model-membrane B, d_{63}-DMPC) a doubled estimated protein insertion occurred. This suggests that the bilayer is hosting a number of channels, giving statistically significant results, We conclude that the protocol for protein delivery to the target membranes was effective, and that this technique can be applied to examine the interaction in other membrane-protein systems. Moreover, it can be appreciated that DSPC serves, as already found in another study [21], as a good supporting membrane for the floating membrane E. It guarantees stability to the system and it is only slightly influenced by the laborious but necessary experimental procedure, resulting only in an expected 5% increase of water volume penetration [20].

Protein insertion induces structural modifications of the membrane. The data also provide important structural information on the specific membrane / channel system, concerning the overall thickness of the hosting membranes and their detailed SLD transmembrane profiles.

Supported membranes A, B, C and D, have a similar bilayer thickness of 44 ± 1 Å. Channel insertion is evident from the change in the contrast profile (Fig. 2); the final thickness of 44 Å is basically unchanged within the experimental error. Differently, the estimated thickness of the floating DPPC *bare* membrane (membrane E) is larger. The insertion of $Kcv_{MA\text{-}1D}$ in this floating membrane causes a major alteration of its SLD profile (Fig. 3). The total average thickness is strongly reduced, from the original 50 Å to 44 Å. This structural change might be caused by a *static* modification in the lipid packing, resulting in *real* membrane thinning of a thick membrane. On the other hand, such a 12% reduction in the evaluated thickness could arise from a *dynamic* effect, that is, a dampening of the undulations affecting the free floating membrane, experimentally detected as an *effective* membrane thinning with respect to an *apparent* original thickness. This dampening of fluctuations could arise from the presence of the embedded channels, acting as defects on the floating membrane meanwhile increasing its average density. Seemingly, the final effect is due to a superposition of the two contributions, *static* and *dynamic*, nonetheless the present data cannot

discriminate between the two explanations. Interestingly, the final thickness after the insertion of the protein is 44 Å for all tested membranes.

Protein insertion into the membrane is directional: structural result. The other main structural information extracted from the reflectivity data, is that, the membrane contrast profile modification is different in the two leaflets. This feature was found in all of the five membranes tested, and for both channels proteins. The *outer* leaflet, exposed to the approaching protein, was always more affected than the inner one. On the other hand, the effect on membrane thickness was the same, as well as the out-leaflet/in-leaflet protein volume penetration ratio (o/i = 1.2). Inspection of the $Kcv_{MA\text{-}1D}$ and Kcv_{NTS} structures (see Figure 1) reveals that they have the shape of a truncated cone, with a 1.2 hindrance ratio between the larger and smaller moieties. In cells, it is assumed that, the largest half, with the turret domain, is oriented towards the extracellular medium and the smaller towards the cytosol. The finding that the membrane is asymmetrically affected by the two conical channels, suggests that the two channels insert with a preferential orientation, namely with the smaller (cytosolic, including the N- and C-termini) side first.

It might be argued that the presence of the silicon support could have a templating effect, imposing the thickness of the lipid/protein membrane, or favouring a preferential insertion of the channel. This hypothesis is ruled out by the experimental data, since we found that the same structural phenomena occur also in the floating membrane. Furthermore the small channels, which were tested here, are so short that they are barely spanning the membrane. They are unlikely interacting with the silicon support.

Directional insertion of the channel proteins in a free membrane constitutes the structural outcome that can be matched by the functional investigation.

3.2 Electrophysiology measurements

Protein insertion into the membrane is directional: electrophysiology result. Electrophysiology experiments were performed on the same channel proteins, functionally reconstituted in planar lipid

bilayers. Fig. 4a shows exemplary current traces of the Kcv_{MA-1D} channel in a L-α-phosphatidylcholine membrane. The channel exhibits a non-symmetrical behaviour. At positive voltages the channel reveals distinct openings with a high open probability. The open probability decreases with negative voltages; at extreme negative voltages the channel opening becomes increasingly noisy and the channel amplitudes even decrease with hyperpolarization. It had been shown in a previous study that the latter phenomenon is caused by a fast gating, which prevents a full resolution of the true open channel amplitude [62]. These experiments also tested that channel functionality was retained after the dialysis procedure.

The product of the unitary single channel I/V relation (Fig. 4b) and the open probability (Fig. 4c) gives the time averaged I/V relation of the Kcv_{MA-1D} channel (Fig. 4d). This I/V curve should reflect the I/V relation of the macroscopic channel current in cells. Previous measurements of Kcv_{MA-1D} in Xenopus oocytes have shown that the channel generates a strong outward rectifier [28]. The comparison of Kcv_{MA-1D} currents in cells with the time averaged I/V relation in the bilayer allows us to define the orientation of Kcv_{MA-1D} in the bilayer. Judging from the rectification of the channel, it can be clearly seen that the channel inserts in an outside-out configuration, with the cytosolic side in the *trans* compartment and the external side in the *cis* compartment. The same outward rectifying I/V relation was observed in seven repeated experiments, thus confirming an orientational preference for the insertion of Kcv_{MA-1D} into the membrane. The channel appeared to insert with the cytosolic part first, in good agreement with a previous study, which reported that a similar channel, Kcv_{PBCV1}, inserts in more than 70% of the cases with the same preference into a phosphatidylcholine bilayer [27].

This finding matches the one independently found by reflectometry, the two techniques being applied to the same experimental model, that of a free phospholipid membrane exposed on one side to an incoming channel protein.

To test if the preferential insertion of the protein is related to the amino acid sequence of the protein we repeated similar electrophysiological experiments with Kcv_{NTS}, in a L-α-phosphatidylcholine

bilayer [52]. Also the Kcv_{NTS} channel exhibits a pronounced asymmetrical activity with a strong flickering of the open channel current at negative voltages [25,29]. This fast gating at extreme negative voltages generates, like in $Kcv_{MA\text{-}1D}$, a decrease in the apparent unitary conductance at negative voltages [29]. In a large number of experiments in which Kcv_{NTS} was reconstituted in a L-α-phosphatidylcholine bilayer the channel exclusively exhibited the same orientation: the flicker like gating of the channel was always observed at negative voltages [29]. When the same experiments were repeated here, the same channel inserted again, in four independent attempts, exclusively uni-directionally into the bilayer; in all cases the negative slope conductance was visible at negative voltages (Fig. 4f). The results of these experiments show that also the second small K^+ channel, namely Kcv_{NTS}, inserts with a strong preference into the bilayer. It is important to note that the same fast gating of the channel and the negative slope are also found at negative voltages when the channel is expressed in Xenopus oocytes [25]. This advocates the same scenario as in the case of the $Kcv_{MA\text{-}1D}$ channel, in that channel inserts with the cytosolic side first.

In further electrophysiology experiments, we tested whether the Kcv_{NTS} channel was also active in a DPPC bilayer, that is, the lipid used in reflectivity experiments. Since it was not possible to obtain stable bilayers of this phospholipid with the standard preparation procedure for conventional horizontal bilayer recordings, we used a modified version of the *Contact Bubble Bilayer (CBB)* method for reconstitution of the Kcv_{NTS} channel in DPPC bilayer (Materials and Methods). The data in Fig. 4e show that this method allowed fabrication of bilayers with active Kcv_{NTS} channels. The activity of the channel was independent of the recording technique, similar in DPPC and DPhPC bilayers. In membranes of both lipids, the channel exhibited a fast flickering with unresolved channel closures. In the present example, this fast gating and the reduction of the apparent unitary conductance is evident at negative voltages (Fig 4e, 4f). The exemplary data in fig. 5e show that the DPPC membrane has an additional effect on Kcv_{NTS}, in that it reduces the unitary conductance of the channel also at positive voltages (Fig. 4e, 4f). This further voltage-dependent effect can be discriminated from the impact on channel gating at negative voltages, since it is not

correlated with a pronounced flickering of the channel. Also with the CBB technique, the time stability of the DPPC bilayers forming at the contact area was only enough for short measurement and it had to be constantly reformed. Thus, it was not possible to obtain unequivocal information based on electrophysiology for a directional insertion of this channel into the DPPC bilayer. In this, the structural result obtained by neutron reflectometry helps in assessing that directional insertion occurs also in this case, and accordingly all the CBB measurements in Fig. 4f are presented such that the fast gating is associated with negative voltages.

Moreover, the present data obtained with different Kcv channels are also similar to previous experiments with the KcsA channel, larger than the Kcv channels. Also KcsA was reported to insert into bilayers with a preferential outside-out configuration [63]. While being only 35% identical in the amino acid composition [64], the KcsA and the Kcv proteins share the same conical shape [26,65]. This suggests that the insertion bias could be determined more by the shape of the protein than by the amino acid composition. In the case of the KscA protein, the bias for a directional insertion into the membrane of small vesicles was claimed to be the shape-matching between the conical shape and the curvature of these vesicles [66]. Reversely, since the present results, both structural and functional, were obtained with planar lipid bilayers, it occurs that there should be factors other than the protein shape contributing to the preferential insertion of the channels into bilayers.

4. Conclusions

In the present study we adapted and combined two typical techniques for studying either membrane structure or ion-channel behaviour to connect structural and functional properties of biomimetic complex environments containing lipids and membrane proteins.

Our electrophysiology experiments showed that the minimal K^+-channel proteins $Kcv_{MA\text{-}1D}$ and Kcv_{NTS} properly inserted into the phospholipid model membranes. Meanwhile, lipid/protein

interaction were monitored by neutron reflectometry detecting structural alterations both in supported and floating membranes.

Following reconstitution of the channel proteins, the mean thickness of the hosting membrane was 44 Å for all of the tested systems, regardless of the initial structure in the absence of protein, consistent with the concept of hydrophobic matching. The fact that structural adaptation occurred in mono-lipid membranes, thus in the absence of any preferential recruitment in the protein environment, supports the notion of structural interference, that is, all components contribute to strategies that avoid hydrophobic mismatch [4,5]. Moreover, besides *static* thickness adaptation, a broader modification of the mechanical properties of the hosting membrane is suggested, resulting in a reduction of the amplitude of the floating membrane fluctuations.

Finally, and notably, neutron reflectometry results directly revealed that the interaction with the phospholipid surface drives the $Kcv_{MA\text{-}1D}$ or Kcv_{NTS} proteins to insert with a specific orientation into the bilayer, namely, the cytosolic half enters first. In this, the structural result matches the functional assay of $Kcv_{MA\text{-}1D}$ and Kcv_{NTS} channels activity, which also stresses a predominant outside-out configuration.

Thus, hybrid approaches emerge as new synergic tools for unravelling structure-function connections of membrane complex platforms.

Acknowledgements

The authors wish to thank the Helmholtz-Zentrum Berlin, and the Institut Laue-Langevin in Grenoble (FR) for beamtime and use of the facilities offered by the Partnership for Soft Condensed Matter (PSCM), and Oliver Rauh (Darmstadt) for testing channel function in planar lipid bilayer after protein dialysis. Work partially supported by grant n. 695078 - noMAGIC, H2020-ERC-2015-AdG to A.M and by grant of the Deutsche Forschungsgemeinschaft to G.T.

References

[1] F. Dumas, M. Chantal Lebrun, J. Tocanne, Is the protein/lipid hydrophobic matching principle relevant to membrane organization and functions?, FEBS Letters 458 (1999) 271-277.

[2] F. Dumas, M. M. Sperotto, M. Lebrun, J. Tocanne, O. Mouritsen, Molecular Sorting of Lipids by Bacteriorhodopsin in Dilauroylphosphatidylcholine/Distearoylphosphatidylcholine Lipid Bilayers, Biophysical Journal 73 (1997) 1940-1953.

[3] T.K.M. Nyholm, S. Özdirekcan, J.A. Killian, How protein transmembrane segments sense the lipid environment, Biochem 46 (2007) 1457-1465.

[4] A. Holt, J.A. Killian, Orientation and dynamics of transmembrane peptides: the power of simple models, Eur Biophys J 39 (2010) 609-621.

[5] J.A. Killian, Hydrophobic mismatch between proteins and lipids in membranes, Biochimica et Biophysica Acta 1376 (1998) 401-415.

[6] F.X. Contreras, A.M. Ernst, F. Wieland,B. Brügger, Specificity of intramembrane protein-lipid interactions, Cold Spring Harb Perspect Biol 3 (2011) a004705.

[7] W. Van Klompenburg, I. Nilsson, G. Von Heijne, B. De Kruijff, Anionic phospholipids are determinants of membrane protein topology, EMBO J. 16 (1997) 4261-4266.

[8] W. Dowhan, M. Bogdanov, Lipid-dependent membrane protein topogenesis, Annu Rev Biochem. 78 (2009) 515-540.

[9] M. Bodganov, P.N. Heacock and W. Dowhan, A polytopic membrane protein displays a reversible topology dependent on membrane lipid composition, The EMBO Journal 21 (2002) 2107-2116.

[10] M. Montal and P.Mueller, Formation of Bimolecular Membranes from Lipid Monolayers and a Study of Their Electrical Properties, PNAS, 69 (1972) 3561-3566.

[11] C. Miller, Ion channel reconstitution. New York: Plenum Press, 1986.

[12] D. De Stefani, A. Raffaello, E. Teardo, I. Szabo and R. Rizzuto, A forty-kilodalton protein

of the inner membrane is the mitochondrial calcium uniporter, Nature 476 (2011) 336-340.

[13] A. Harsman, P. Bartsch, B. Hemmis, V. Krüger, R. Wagner, Exploring protein import pores of cellular organelles at the single molecule level using the planar lipid bilayer technique, Eur. J Cell Biol. 90 (2011) 721-730.

[14] J. Popot, Amphipols, nanodiscs, and fluorinated surfactants: three nonconventional approaches to studying membrane proteins in aqueous solutions, Ann Rev Biochem, 79 (2010) 737-735.

[15] S. Inagaki, R. Ghirlando, R. Grisshammer, Biophysical characterization of membrane proteins in nanodiscs, Methods, 59 (2013) 287-300.

[16] J. Borch, T. Hamann, The nanodisc: a novel tool for membrane protein studies, Biol Chem, 390 (2009) 805-814.

[17] T.H. Bayburt and S.G. Sligar, Membrane protein assembly into Nanodiscs, FEBS Letters, 584 (2010) 1721-1727.

[18] H.P. Vacklin, F.Tiberg, G. Fragneto, R.K. Thomas, Composition of supported model membranes determined by neutron reflection, Langmuir 21 (2005) 2827-2837.

[19] V. Rondelli, P. Brocca, S. Motta, M. Messa, L. Colombo, M. Salmona, G. Fragneto, L. Cantù, E. Del Favero, Amyloidβ Peptides in interaction with raft-mime model membranes: a neutron reflectivity insight, Scientific Reports 6 (2016) 20997.

[20] V. Rondelli, G. Fragneto, S. Motta, E. Del Favero, P. Brocca, S. Sonnino and L. Cantù, Ganglioside GM1 forces the redistribution of cholesterol in a biomimetic membrane, BBA-Biomembranes 1818 (2012) 2860-2867.

[21] V. Rondelli, E. Del Favero, S. Motta, L. Cantù, G. Fragneto, P. Brocca, Neutrons for rafts, rafts for neutrons, Eur. Phys. J. E 36 (2013) 13073.

[22] D. J. McGillivray, G. Valincius, F. Heinrich, J.W.F. Robertson, D. J. Vanderah, W. Febo-Ayala, I. Ignatjev, M. Lösche, J.J. Kasianowicz, Structure of Functional Staphylococcus aureus α-Hemolysin Channels in Tethered Bilayer Lipid Membranes, Biophys J. 96 (2009) 1547–1553.

[23] S. Krueger, Neutron reflection from interfaces with biological and biomimetic materials, Current Opinion in Colloid & Interface Science, 6 (2001) 111-117.

[24] T. Charitat, E. Bellet-Amalric, G. Fragneto, F. Graner, Adsorbed and free lipid bilayers at the solid-liquid interface, E Phys J B 8 (1999) 583-593.

[25] S. Gazzarrini, M. Kang, A. Abenavoli, G. Romani, C. Olivari, D. Gaslini, G. Ferrara, J. L. van Etten, M. Kreim, S. M. Kast, G. Thiel, A. Moroni, Chlorella virus ATCV-1 encodes a functional potassium channel of 82 amino acids, Biochemical Journal420 (2009) 295-303.

[26] S. Tayefeh, T. Kloss, G. Thiel, B. Hertel, A. Moroni, S. Kast, Molecular dynamics simulation of the cytosolic mouth in Kcv-type potassium channels, Biochemistry 46 (2007) 4826-4839.

[27] C. Pagliuca, T.A. Goetze, R. Wagner, G. Thiel, A. Moroni, D. Parcej, Molecular properties of Kcv, a virus encoded K+ channel, Biochemistry 46 (2007) 1079-1090.

[28] S. Gazzarrini, M. Kang, J.L.Van Etten, S. Tayefeh, S.M. Kast, D. DiFrancesco, G. Thiel, A. Moroni, Long-distance interactions within the potassium channel pore are revealed by molecular diversity of viral proteins, J. Biol. Chem. 279 (2004) 28443-28449.

[29] O. Rauh, M. Urban, L.M. Henkes, T. Winterstein, T. Greiner,J.L. Van Etten, A. Moroni, S.M. Kast, G. Thiel, I. Schroeder, Identification of Intrahelical Bifurcated H-Bonds as a New Type of Gate in K+ Channels, J. Am. Chem. Soc. 139 (2017) 7494-7503.

[30] M. Kang, A. Moroni, S. Gazzarrini, D. DiFrancesco, G. Thiel,M. Severino, J.L Van Etten, Small potassium ion channel proteins encoded by chlorella viruses, Proc Natl Acad Sci U S A 101 (2004) 5318-5324.

[31] F. Hoffgaard, S.M. Kast, A. Moroni, G. Thiel, K. Hamacher, Tectonics of a K^+ channel: The importance of the N-terminus for channel gating, Biochim. Biophys. Acta 1848 (2015) 3197-3204.

[32] S. Tayefeh, T. Kloss, G. Thiel, B. Hertel, A. Moroni, S. Kast, Molecular dynamics simulation of the cytosolic mouth in Kcv-type potassium channels, Biochemistry 46 (2007) 4826-4839.

[33] UCSF Chimera, https://www.cgl.ucsf.edu/chimera/, last accessed on April 2018

[34] M. le Maire, P. Champeil, J. V. MÖller, Interaction of membrane proteins and lipids with solubilizing detergents, Biochimica et Biophysica Acta 1508 (2000) 86-111.

[35] B. Madler, H. Binder, G. Klose, Compound Complex Formation in Phospholipid Membranes Induced by a Nonionic Surfactant of the Oligo(ethylene oxide) –Alkyl Ether Type: A Comparative DSC and FTIR Study, Journal of Colloid and Interface Science 202 (1998) 124–138.

[36] S. E. Schullery, T. A. Seder, D. A. Weinstein, D. A. Bryant, Differential Thermal Analysis of Dipalmitoylphosphatidylcholine-Fatty Acid Mixtures, Biochemistry 20 (1981) 6818-6824.

[37] K. Gawrisch, L. L. Holte, NMR investigations of non-lamellar phase promoters in the lamellar phase state, Chemistry and Physics of Lipids 81 (1996) 105-116.

[38] J. R. Henriksen, T. L. Andresen, L. N. Feldborg, L. Duelund, J. H. Ipsen, Understanding Detergent Effects on Lipid Membranes: A Model Study of Lysolipids, Biophysical Journal, 98 (2010) 2199–2205.

[39] A. M. Seddon, P. Curnow, P.J. Booth, Membrane proteins, lipids and detergents: not just a soap opera, Biochimica et Biophysica Acta 1666 (2004) 105 – 117.

[40] R.M. Garavito, S. Ferguson-Miller, Detergents as tools in membrane biochemistry, J. Biol. Chem. 276 (2001) 32403 – 32406.

[41] Y. Gohon, J. Popot, Membrane protein–surfactant complexes, Current Opinion in Colloid and Interface Science 8 (2003) 15–22

[42] L. Rosa, S. Scalisi, F. Lolicato, M. Pannuzzo, A. Raudino, Lipid-assisted protein transport: A diffusion-reaction model supported by kinetic experiments and molecular dynamics simulations, J. Chem. Phys. 144 (2016) 184901.

[43] V. Rondelli, P. Brocca, N. Tranquilli, G. Fragneto, E. Del Favero, L. Cantù, Building a biomimetic membrane for neutron reflectivity investigation: Complexity, asymmetry and contrast, Biophysical Chemistry, 229 (2017) 135-141.

[44] L.D. Mayer, M.J. Hope, P.R. Cullis, Vesicles of variable sizes produced by a rapid

extrusion procedure, BBA, 858 (1986) 161-168.

[45] B. Seantier, C. Breffa, O. Felix, G. Decher, In Situ Investigations of the Formation of Mixed Supported Lipid Bilayers Close to the Phase Transition Temperature, NANO Letters 4 (2004) 5-10.

[46] G. Roberts, Langmuir Blodgett films, Plenum press New York, 1990.

[47] L.K. Tamm, H.M. McConnell, Supported phospholipid bilayers, Biophys. J. 47 (1985) 105-113.

[48] V. Rondelli , G. Fragneto, S. Motta, E. Del Favero, L. Cantù, Reflectivity from floating bilayers: can we keep the structural asymmetry?, Journal of Physics: conference series 340 (2012) 012083

[49] R. Cubitt , G. Fragneto, D17: the new reflectometer at the ILL, Applied Physics A 74 (2002) s329-s331.

[50] M. Trapp, R. Steitz, M. Kreuzer, M. Strobl, M. Rose, R. Dahint, BioRef II—Neutron reflectometry with relaxed resolution for fast, kinetic measurements at HZB, Review of Scientific Instruments 87 (10) (2016) 105112.

[51] J. Penfold, R.K. Thomas, The application of specular reflection of neutrons to the study of surfaces and interfaces, JPCM 2 (1990) 1369.

[52] C.J. Braun, C. Lachnit, P. Becker, L.M. Henkes, C. Arrigoni, S.M. Kast, A. Moroni, G. Thiel,I. Schroeder, Viral potassium channels as a robust model system for studies of membrane-protein interaction, Biochim. Biophys. Acta 1838 (2014) 1096-1103.

[53] L.M. Winterstein, K. Kukovetz O.Rauh, , D.L. Turman C.Braun, , A.Moroni, I., Schroeder, G.Thiel, Reconstitution and functional characterization of ion channels from nanodiscs in lipid bilayers, J. Gen Physiol. 150 (2018) 637-646.

[54] M. Iwamoto, S. Oiki, Contact Bubble Bilayers with Flush Drainage, Nature Scientific Reports 5 (2015) 9110.

[55] L.D. Mosgaard, T. Heinburg, Lipid Ion Channels and the Role of Proteins, Accounts of Chemical Research 46 (2013) 2966-2976.

[56] E.B. Watkins, C.E. Miller, D.J. Mulder, T.L. Kuhl, J. Majewski, Structure and Orientational Texture of Self-Organizing Lipid Bilayers, Phys Rev Lett 102 (2009) 238101.

[57] C.E. Miller, D.D. Busath, B. Strongin, J. Majewski, Integration of Ganglioside GT1b Receptor into DPPE and DPPC Phospholipid Monolayers: An X-Ray Reflectivity and Grazing-Incidence Diffraction Study, Biophys Journal 95 (2008) 3278-3286.

[58] J. F. Nagle, S. Tristram-Nagle, Structure of lipid bilayers. BBA 1469 (2000) 159-195.

[59] J. Daillant, E. Bellet-Amalric, A. Braslau, T. Charitat, G. Fragneto, F. Graner, S. Mora, F. Rieutord, B. Stidder, Structure and fluctuations of a single floating lipid bilayer, PNAS 102 (2005) 11639-11644.

[60] B. Stidder, G. Fragneto, S.J. Roser, Effect of low amounts of cholesterol on the swelling behavior of floating bilayers, Langmuir, 21 (2005) 9187-93.

[61] A. Nelson, Co-refinement of multiple-contrast neutron/X-ray reflectivity data using MOTOFIT, Journal of Applied Crystallography 39 (2006) 273-276.

[62] A. Abenavoli, M. DiFrancesco, I. Schroeder, S. Epimashko, S. Gazzarrini, U.P. Hansen,G. Thiel, A. Moroni, Fast and slow gating are inherent properties of the pore module of the K+ channel Kcv, J. Gen. Physiol. 134 (2009) 219-229.

[63] L.G. Cuello, J.G. Romero, D.M. Cortes, E. Perozo, pH-dependent gating in the Streptomyces lividans K+ channel, Biochemistry 37 (1998) 3229-3236.

[64] B. Plugge, S. Gazzarini, R. Cerana, J. Van Etten, M. Nelson, D. Di Francesco, A. Moroni, G. Thiel, A Potassium Channel Protein Encoded by Chlorella Virus PBCV-1, Science 287 (2000) 1641-1644.

[65] D.A. Doyle, C.J. Morais , R.A. Pfuetzner, A. Kuo, J.M. Gulbis, S.L. Cohen, B.T. Chait, R. MacKinnon, The structure of the potassium channel: molecular basis of K+ conduction and selectivity, Science 280 (1998) 69-77.

[66] M. Yanagisawa,M. Iwamoto,A. Kato,K. Yoshikawa, S. Oiki, Oriented reconstitution of a membrane protein in a giant unilamellar vesicle: experimental verification with the potassium channel KcsA, JACS 133 (2011) 11774-11779.

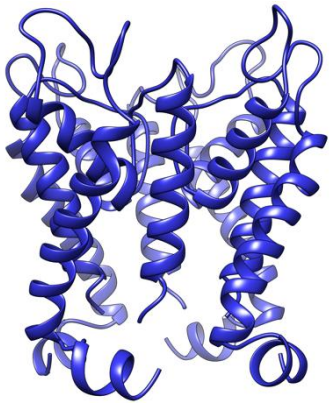

Figure 1 Structure of the Kcv channel protein. The image shows the tetrameric ensemble of $Kcv_{PBCV\text{-}1}$ (95% sequence identity to $Kcv_{MA\text{-}1D}$). A similar structure was obtained for Kcv_{NTS} [29]. The overall shape is that of a truncated cone, with approximately 1.2 hindrance ratio between the larger and the smaller moieties.

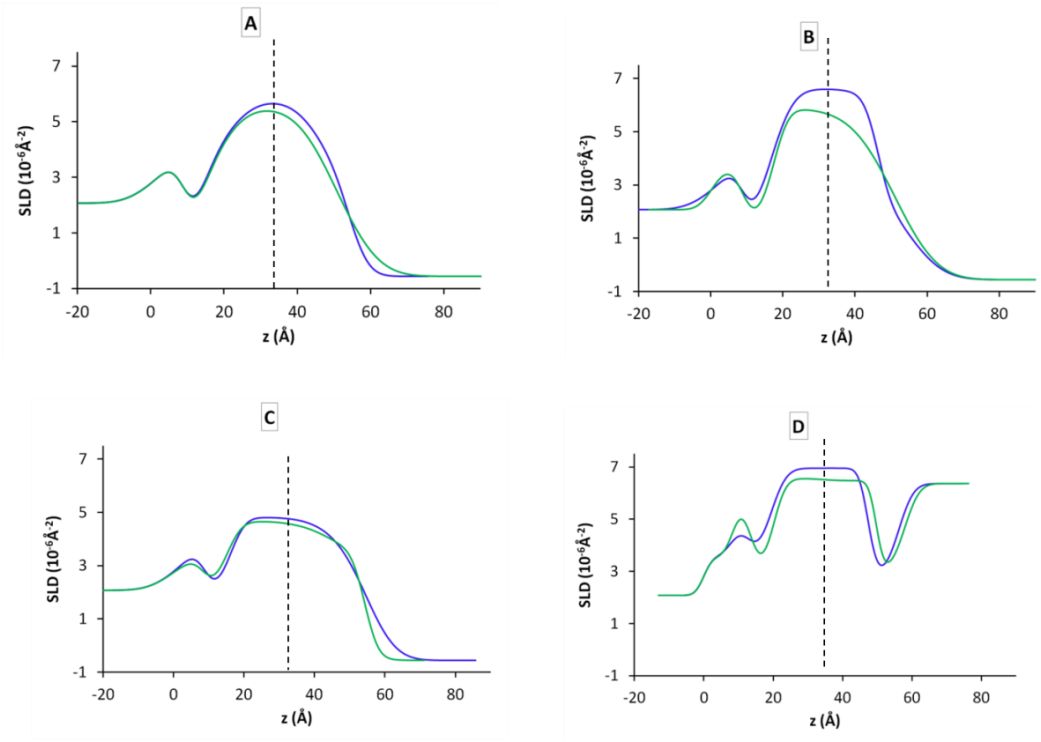

Figure 2 Scattering Length Density profiles of the four supported membranes investigated before (blue) and after (green) interaction with Kcv channels in H_2O (A, B and C) or in D_2O (D). A: d_{63}-DMPC (membrane A), T=40°C; B: d_{63}-DMPC (membrane B) then incubated with doubled amount of protein, T=40°C; C: d_{75}-DPPC (membrane C), T=45°C; D: d_{62}-DPPC (membrane D), T=45°C. The z(Å) axis refers to the distance from the silicon support. The dotted vertical lines indicate membranes mid-planes.

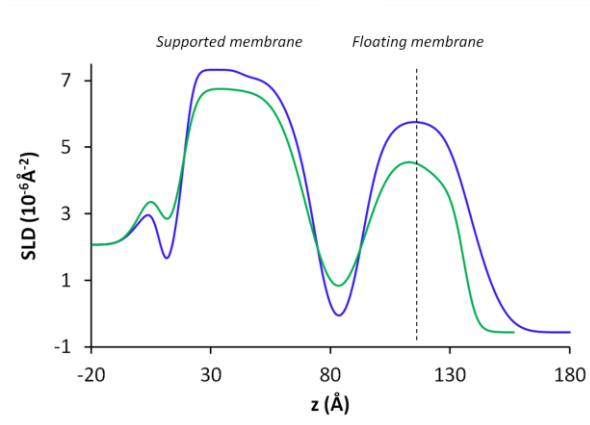

Figure 3 Scattering Length Density profiles of the two-membrane system E investigated before (blue) and after (green) interaction with Kcv channel in H_2O at T=45°C. The supported membrane is composed by d_{83}-DSPC and the floating by d_{75}-DPPC. The z(Å) axis refers to the distance from

the silicon support. The dotted vertical line indicates roughly the mid-plane of the floating membrane.

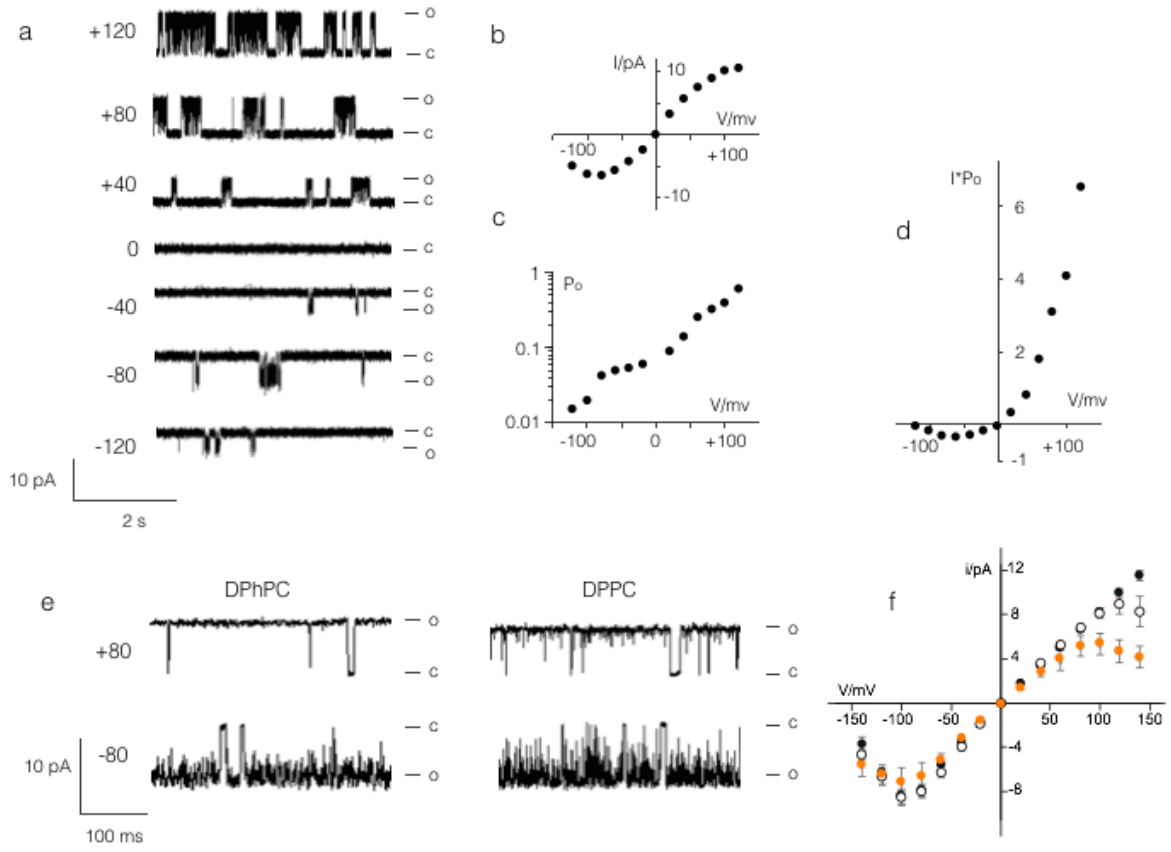

Figure 4 Single channel fluctuations of $Kcv_{MA\text{-}1D}$ (a, b, c, d) and Kcv_{NTS} (e, f) channels in phosphocholine bilayers. (a) Functional reconstitution of $Kcv_{MA\text{-}1D}$ in horizontal planar lipid DPhPC bilayer. Representative channel fluctuations between open (o) and closed (c) states in symmetrical 100 mM KCl solution at voltages between +120 mV and -120 mV with corresponding I/V relation (b) and open probability as function of voltage (c). The product of the single channel amplitude from (b) and the open probability from (c) (i·Po) provides the time averaged I/V relation in (d) with a strong outward rectification. (e) Representative channel fluctuations of Kcv_{NTS} in DPhPC and DPPC bilayer recorded at + 80 mV and -80 mV with the CBB technique. The corresponding I/V relations are summarized in (f): from n = 8 independent measurements under the same conditions in DPPC (orange symbols); from n = 5 measurements in DPhPC bilayers (open symbols). The data obtained with the standard horizontal-bilayer method in DPhPC are also

reported for comparison (full symbols, n = 4). Measurements were always performed in symmetrical 100 mM K^+ buffer. Data in (f) are mean ± standard deviation.

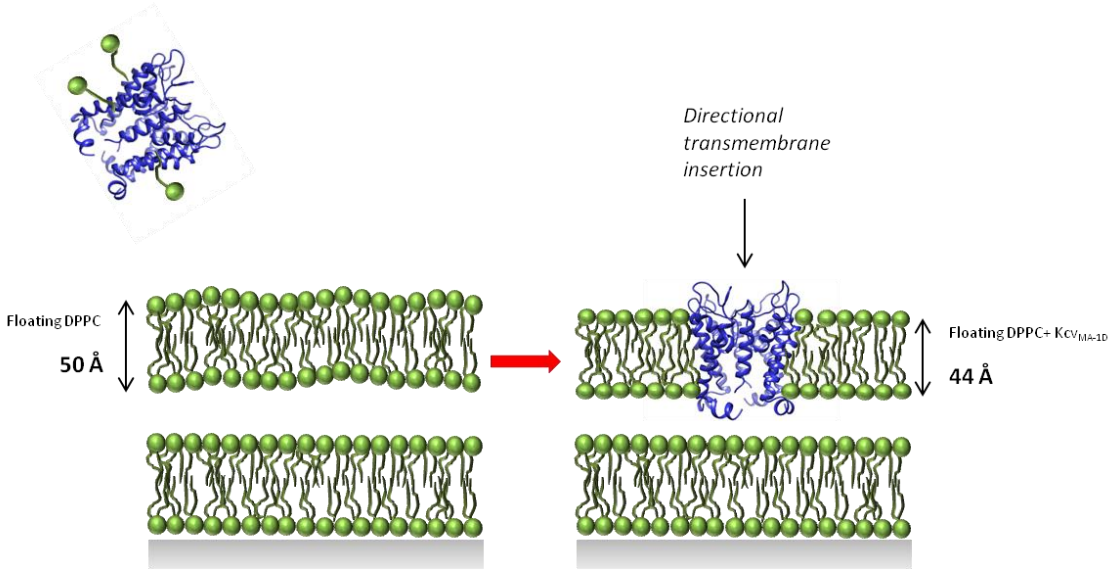

Graphical abstract Kcv protein inserts with a preferential orientation in model membranes, inducing a favourable hydrophobic match between protein and bilayer and dampening membrane oscillations.